Temperature dependent extension of a static hysteresis model

Fabien Sixdenier, Oualid Messal, Alaa Hilal, Christian Martin, Marie-Ange Raulet, Riccardo Scorretti

Temperature dependent extension of a static hysteresis model

Fabien Sixdenier, Oualid Messal, Alaa Hilal, Christian Martin, Marie-Ange Raulet and Riccardo Scorretti

Some soft magnetic materials are strongly dependent of the temperature, because of their low Curie temperature. In order to predict their behavior in electrical devices, engineers need hysteresis models able to take into account the temperature. This paper is an attempt to take into account the temperature in an existing model of static hysteresis through its parameters. Variations of some parameters with temperature are issued or build thanks to the literature. At the end, all needed parameters have an analytical law versus temperature. Simulation results are compared to measurements and discussed.

***Index Terms*—Temperature dependance, magnetic hysteresis, thermal stresses,...**

I. Introduction

In order to reduce the volume/mass of soft magnetic materials in electrical devices, there are most likely two main solutions: increase the "working" induction level $\widehat{B}$ or the frequency f. The both solutions lead to increase the magnetic losses p_{mag} of the device and consequently increase the temperature T, due to self heating. Moreover, soft magnetic materials that have a low Curie temperature T_c are strongly dependent on the temperature and this behavior is highly non-linear. Thus, designers need models able to predict the magnetic behavior in a "large" temperature range (from 25 °C to T_c). In this aim, the authors of [1], [2], used the static Jiles-Atherthon (JA) model with different parameter variation laws (analytical and/or numerical). Thanks to analytical laws [3] and optimization methods, a good compromise between the error levels and the monotony of the parameters is achieved in [4]. Nevertheless, for complex induction $b(t)$ waveforms, JA model generally fails to predict excitation field $h(t)$ with accuracy due to several intrinsic, well detailed in [5]. Engineers need, then, a reliable static hysteresis model able to take into account both complex inductions waveforms and the temperature influence on the magnetic material properties. To achieve this goal, an adaptation of an existing hysteresis model called Vector-Play Model (VPM) [6] is proposed in this paper. We chose to test this approach on an alloy, named Phyterm260 commercialized by the APERAM company [7]. This alloy is normally dedicated to induction cookwares. It is a $Ni_{50}Fe_{bal}Cr_9$ alloy with a Curie temperature around 260 °C. The VPM has been tested and implemented in finite elements by many authors [8], [9] and recently been improved in [10] in the case of rotating fields. The same authors also proposed, in [11], a method where they considered, linear variations of saturation magnetization and coercive field to take into account the temperature for permanent magnets. In this paper, a brief reminder of the VPM is first presented in order to define some variables that will be used in the temperature dependent extension. Then the temperature dependent extension is introduced associated to its parameters identification protocol for soft magnetic materials. Finally, the robustness of the model is tested with complex signals and temperatures that are not part of the identification protocol. The ability of the developed model to qualitatively retrieve the Hopkinson effect [12] is also tested. Simulations are compared to measurements that were performed on ring samples wound with high temperature enameled wires (placed in an oven) following the fluxmetric method with respect to the IEC 60404-4 standard [13].

Paper sent on June 2015 for peer review

Fabien Sixdenier, Alaa Hilal, Christian Martin, Marie-Ange Raulet and Riccardo Scorretti are working at Université de Lyon, Université Lyon 1, CNRS UMR5005 AMPERE, France, emails : fabien.sixdenier@univ-lyon1.fr, alaa.hilal@univ-lyon1.fr, christian.martin@univ-lyon1.fr, marie-ange.raulet@univ-lyon1.fr, Riccardo.Scorretti@univ-lyon1.fr

Oualid Messal is working at Grenoble INP - UJF Grenoble 1 - CNRS UMR 5269 (G2Elab), France, email : oualid.messal@g2elab.grenoble-inp.fr

corresponding author: Fabien Sixdenier

II. Vector Play Model

A. Original Model

The evaluation of magnetization $\mathbf{M}$ from the applied field $\mathbf{h}$ is performed in two steps. First, the vector play operator $\mathbf{h}_{re}$ has to be evaluated with (1), with χ linked to the coercivity, $\mathbf{h}$ the applied field and $\mathbf{h}_{re0}$ the initial value of $\mathbf{h}_{re}$. In (1), the applied field $\mathbf{h}$ is decomposed into a reversible part $\mathbf{h}_{re}$ and an irreversible part $\mathbf{h}_{ir}$. Fig 1 shows the vector diagram in each case.

$$\mathbf{h}_{re} = \begin{cases} \mathbf{h}_{re0} & \text{if} |\mathbf{h}-\mathbf{h}_{re0}| < \chi \\ \mathbf{h} - \chi \cdot \frac{\mathbf{h}-\mathbf{h}_{re0}}{|\mathbf{h}-\mathbf{h}_{re0}|} & \text{if} |\mathbf{h}-\mathbf{h}_{re0}| \geq \chi \end{cases} \quad (1)$$

Fig. 1. Vector diagram for vector play operator in 2 cases: $|\mathbf{h}-\mathbf{h}_{re0}| < \chi$ (left) ; $|\mathbf{h}-\mathbf{h}_{re0}| \geq \chi$ (right)

Then the magnetization $\mathbf{M}$ is calculated thanks to (2), where $M_{an}(h_{re})$, is the anhysteretic curve and h_{re} is the absolute value of $\mathbf{h}_{re}$.

$$\mathbf{M} = M_{an}(h_{re}) \cdot \mathbf{h}_{re}/h_{re} \quad (2)$$

Finally, the induction $\mathbf{b}$ is obtained by solving (3)

$$\mathbf{b} = \mu_0 \cdot (\mathbf{h} + \mathbf{M}) \quad (3)$$

Qualitative interesting results for major loops are given by VPM, in this way. In order to improve the model accuracy,

the magnetization $\mathbf{M}$ can be separated into several parts $\mathbf{M^k}$ that have their own χ^k. Each $\mathbf{M^k}$ associated to χ^k will now be called a cell. If ω^k are the the fraction coefficients, then $\sum_{k=1}^{N} \omega_k = 1$ and $\omega^k \mathbf{M} \equiv \mathbf{M^k}$ are properties that have to be respected. For each cell, the first step is still valid and implies (4).

$$\mathbf{h} = \mathbf{h}_{re}^k - \mathbf{h}_{ir}^k \tag{4}$$

Each cell is tested independently and each $\mathbf{h}_{re}^k$ depending on each χ^k is calculated. Then the global magnetization $\mathbf{M}$ is calculated by (2) with $\mathbf{h}_{re} = \sum_{k=1}^{N} \omega_k \mathbf{h}_{re}^k$.

B. Parameters identification

1) Anhysteretic function

The model is vectorial and so able to deal with rotating fields or ellipsoidal fields, but it is generally easier to identify the parameters for alternating fields. In this paper, all the applied fields $\mathbf{h}$ are unidirectional, so the magnetic magnetization $\mathbf{M}$ is automatically in the same direction. The magnetization $\mathbf{M}$ is calculated thanks to (2), where $M_{an}(h_{re})$, is the anhysteretic curve. Even if the model is phenomenological, it makes sense to use some functions and parameters from physics of ferromagnetism. In paramagnetic materials, $\mathbf{M}$ is generally estimated by the "Langevin" function (5).

$$\mathbf{M} = M_s \left(\coth\left(\frac{|\mathbf{H}|}{a}\right) - \frac{a}{|\mathbf{H}|} \right) \cdot \frac{\mathbf{H}}{|\mathbf{H}|} \tag{5}$$

M_s is the saturation magnetization at a given temperature, $\mathbf{H}$ is a local magnetic field and a is a shape parameter. Let's also remember that $a = k_B T/(\mu_0 m)$, with $k_B \approx 1.38 \cdot 10^{-23}$ J/K, the Boltzmann constant, $\mu_0 = 4\pi \cdot 10^{-7}$ H/m, the vacuum permeability and m the effective atomic magnetic moment. For ferromagnetic materials, the local magnetic field is assumed as $\mathbf{H} = \mathbf{h} + \alpha \mathbf{M}$, with α, the molecular field constant in the Weiss mean field theory [3]. It means that the applied field $\mathbf{h}$ in (1) has to be replaced by $\mathbf{H}$. For a given temperature, three parameters (M_s, α and m) have to be identified. This will be discussed in another section.

2) Cell separation

As said earlier, the model accuracy can be improved if the magnetization $\mathbf{M}$ is separated into several parts that have their own χ^k. The authors of [8] have shown that the accuracy is improved by increasing the number of cells. However, a number of cells superior to 8 did not improve the accuracy significantly anymore. For these reasons, we chose 7 as a reasonable number of cells. The last cell should be reserved to represent an image of the coercive field H_c (obtained on a major loop). In this case, $\chi^{last} = H_c$. One can write $\mathbf{M} = \sum_{k=1}^{N} \omega_k \mathbf{M}$ and $\chi^k = p_k H_c$ (with $0 < p_k < 1$, a weight parameter). It makes sense to assume that $\chi^1 = 0$ associated to $\omega_1 \mathbf{M}$, would represent the reversible magnetization (bending of Bloch walls). The different weights (ω_k and p_k) can be identified thanks to the $h_{coer}(h_{peak})$ [9] and $M_{peak}(h_{peak})$ curves. These curves are traced by measuring symmetrical loops with increasing values of h_{peak} (amplitude of applied field). The relative $h_{coer}(h_{peak})$ and $M_{peak}(h_{peak})$ curves look approximately the same (see Fig. 2 (left)) in the case of this material. The weights ω_k and p_k have to be adjusted in order to fit as best as possible the $M_{peak}(h_{coer})$ curve (see Fig. 2 (right)).

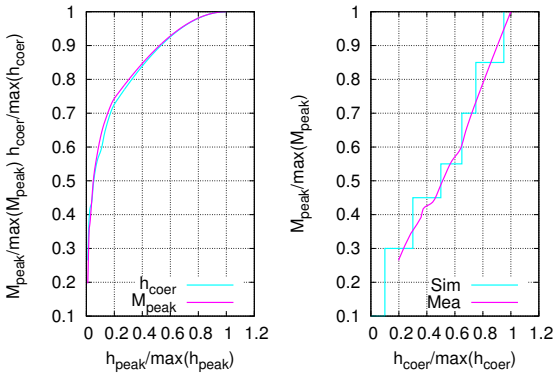

Fig. 2. left figure: Measured per unit $h_{coer}(h_{peak})$ and $M_{peak}(h_{peak})$ curves ; right figure: $M_{peak}(h_{coer})$ measured (Mea) and simulated (Sim) curves

After identification, the ω_k and p_k coefficients are shown in table I. It is assumed, after this section, that all ω_k and p_k are independent of the temperature.

TABLE I
ω_k AND p_k VALUES

k	1	2	3	4	5	6	7
ω_k	0.1	0.2	0.15	0.1	0.15	0.15	0.15
p_k	0	0.1	0.3	0.5	0.6	0.7	1

III. Temperature dependent extension

All equations and principles of the model seen before remain valid, only some parameters will have their value changed. This section is devoted to find analytical/numerical relations of some parameters with temperature. All results of identification are reported in the table II.

A. Saturation Magnetization M_s

As the saturation magnetization M_s of a ferromagnetic material can be assumed to be function of the temperature T following the law (6) [3], with M_{s0} the magnetization at $T = 0$ K and T_c the Curie temperature.

$$\frac{M_s}{M_{s0}} = \tanh\left(\frac{M_s/M_{s0}}{T/T_c}\right) \tag{6}$$

The value of M_s, at a given temperature, is calculated with (6) and its value is used in (5). A few measured major loops at different temperatures in order to identify M_{s0} and T_c with accuracy were necessary.

B. Molecular field constant α and effective atomic magnetic moment m

Anhysteretic curves extracted from measured major loops can be compared to those calculated by (5) where both m and

α are present in the equation. For a given temperature, the previous unknown M_s in (5) is now calculated by (6). One has to identify m and α to minimize the error between the measured and simulated anhysteretic curves. Weiss showed, in [3], that the calculation of the energy of magnetization at $T \approx 0$ K and at high temperatures with $\alpha = cte$ give values that agree with those deduced from measurements of specific heats of pure nickel element. He concluded that α was independent:

- of the applied field
- of the temperature

Thus, we assume in the following that α can be considered as constant in the whole range of temperature ($0 < T < T_c$). In [14] the effective atomic magnetic moment m is assumed to depend on temperature, volume and external magnetic field for temperatures close to T_c. In the empirical model developed by the author, a constant of the main equation depends on the density of states of the 3d-electron bands. For engineering purposes, the needed data of this approach are mostly unavailable. Nevertheless, the author mentioned that far above the Curie point, m was "stable" with temperature but that the change in volume near the Curie point (spontaneous volume magnetostriction) was sufficiently enough to modify the "apparent" atomic magnetic moment. In [1], the authors made the assumption that a showed an exponential decay with temperature such as $a = a_0 \exp^{-T/(\gamma T_c)}$ (with a_0 the value of a at $T = 0$ K). With this assumption and knowing that $a = k_B T/(\mu_0 m)$, one can identify m as (7).

$$m = \frac{k_B T}{\mu_0 a_0} \exp^{T/(\gamma T_c)} \tag{7}$$

C. Coercive field H_c

As said earlier, $\chi^k = p_k H_c$, and the weight parameters p_k are kept constant with temperature. One has just to identify the evolution of the coercive field H_c with temperature and find an analytical law to represent its behavior. In [10], the authors assumed linear dependance of H_c versus temperature because the maximum temperature tested in their case was far above the Curie temperature of the permanent magnet tested (Sm_2Co_{17}, $T_{max} = 150$°C, $T_c \approx 800$°C). As our need is to simulate the behavior of our magnetic material from 25°C to Curie temperature , this approach can not be applied. In [1], the authors chose an exponential decay with temperature of the parameter representing the coercive field (8), with H_{c0}, the coercive field at $T = 0$ K and β the exponential decay coefficient.

$$H_c = H_{c0} \exp^{-T/(\beta T_c)} \tag{8}$$

D. Parameters evolution with temperature

This subsection resumes the parameters M_s, m and α, evolution with temperature obtained with the protocol mentioned above. All the needed values mentioned in (6), (7) and (8) are reported in the table II. Fig. 3 shows the per unit variations of M_s, m and H_c versus temperature. One can see that the measured values of M_s and H_c are in good agreement with those calculated by (6) and (8) respectively. Fig. 3 also shows that the calculated atomic magnetic moment slowly increases for very low temperatures (linear dependance $k_B T/(\mu_0 a_0)$ part) showing a "stable" value [14], then increases very fast when $T > 200$ K. We observed that simulated anhysteretic curves were very sensitive to m and α. We checked that, when m and α were fitted as free parameters, the obtained values were very close to the ones computed analytically, and the shape of the anhysteretic curves were not modified significantly: this justifies the use of the analytical expressions instead of a "brute force" numerical fit.

TABLE II
PARAMETERS VALUES

M_{s0} (kA/m)	T_c (K)	α	a_0 (A/m)	γ	H_{c0} (A/m)	β
674.65	543	1.275e-4	121	0.464	15.55	0.768

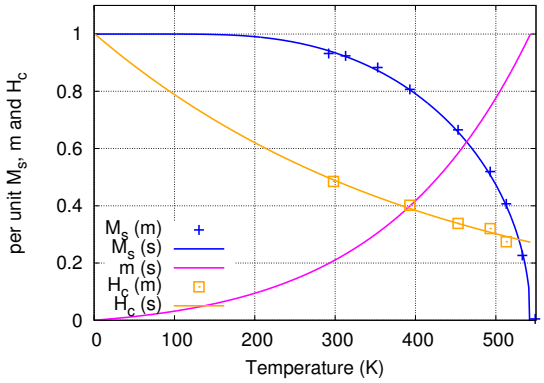

Fig. 3. Per unit variations of M_s, m and H_c versus temperature ((m): measured values), (s): simulated values)

IV. RESULTS

A. Major loops

Fig. 4 shows the measured and simulated major loops at different temperatures. The simulated hysteresis loops are globally in good agreement with the the measured ones. The $L1$ norm ϵ between the measured and simulated loops was $4.11 < \epsilon < 8.73$ % within the temperature range.

B. "Complex" signals and temperature

In order to test the model in "complex" conditions, the applied field waveform is as $h(t) = 4\left(\sin(\omega t) + sin(3\omega t)\right)$. The model had no problem to simulate harmonics (closed small loops at the tips of each loop at a given temperature in Fig.5) as it has already been shown in [8] . However, the simulated levels of b, for the same h input, are not respected. First (2) is not a good approximation of the measured anhysteretic curve (for this material). Second, m, γ and α parameters have been identified thanks to major loops with an amplitude much higher than the test signals (ratio of 66). In Fig. 5, starting from the loop at $T = 25°$ C, the loops first expand ($T = [110, 160]°$ C) when heating then shrink ($T = [220, 240]°$ C). This is true for the both simulated and

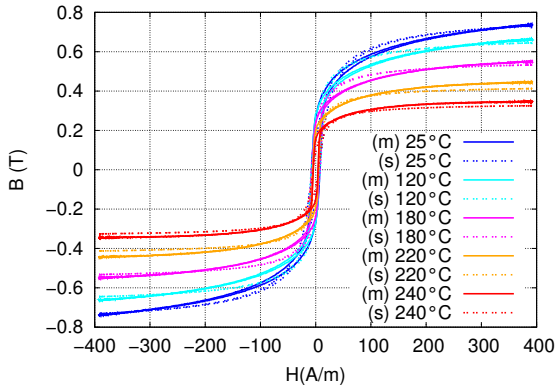

Fig. 4. Measured (m) and simulated (s) major loops at different temperatures

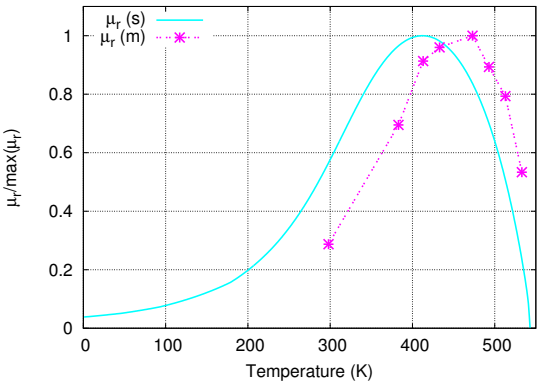

Fig. 6. Measured (m) and simulated (s) per unit magnetic permeability versus temperature

measured loops showing that the evolution of the parameters combined to the model is able to predict the thermal behavior of the material.

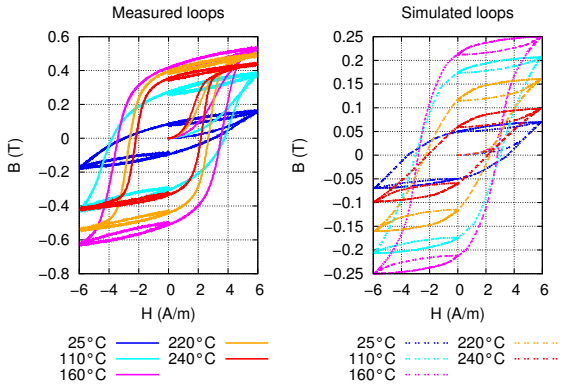

Fig. 5. Measured and simulated "complex" loops at different temperatures

C. Hopkinson effect

Fig. 6 shows the measured (m) and simulated (s) per unit magnetic permeability versus temperature. It can be seen that the shapes of the two curves are similar, but the measured curve is shifted on the high temperatures. The same behavior has been observed in Fig. 5, where after $T = 160°\text{C}$, the loops start to shrink but slower in the case of the measured loops.

V. Conclusion

In this paper, a first attempt to take into account the temperature in an existing hysteresis model has been made. The purely magnetic behavior $b(h)$ showed some errors for "complex" low amplitude signals. These errors could be explained by (5) used to approximate measured anhysteretic curves, which is known to be not so accurate. Accuracy might be improved by interpolating measured anhysteretic curves at different temperatures $M_{an}(h, T)$, but this "black-box solution" will hide the physics of the model. However the Vector Play Model (VPM) showed no difficulties to adapt itself to the temperature dependence, by allowing some parameters to change their values. The thermal behavior is qualitatively well retrieved, loops expand or shrink themselves in function of temperature showing the ability of the build model to retrieve the Hopkinson effect. Some other materials, like ferrites ($T_c \approx 250°\text{C}$), have to be tested, in order to know if this approach can be generalized.

References

[1] A. Raghunathan, Y. Melikhov, J. E. Snyder, and D. Jiles, "Theoretical model of dependence of hysteresis based on mean field theory," *IEEE Transactions on Magnetics*, vol. 46, no. 06, p. 1507 –1510, 2010.

[2] O. Messal, F. Sixdenier, L. Morel, and N. Burais, "Temperature dependent extension of the jiles-atherton model: Study of the variation of microstructural hysteresis parameters," *IEEE Transactions on Magnetics*, vol. 48, no. 10, pp. 2567–2572, 2012.

[3] P. Weiss, "La constante du champ moléculaire. equation d'état magnétique et calorimétrie," *Journal de Physique*, vol. 1, no. 5, pp. 163–175, 1930.

[4] O. Messal, F. Sixdenier, L. Morel, and N. Burais, "Thermal behavior of iron-nickel-chromium alloys and correlation with magnetic and physical properties - part a: Static effects modeling," in *Proceedings of the 19th Conference on the Computation of Electromagnetic Fields*. Budapest : Hungary: Compumag 2013, July 2013.

[5] S. Zirka, Y. Moroz, R. Harrison, and K. Chwastek, "On physical aspects of the jiles-atherton hysteresis models," *JOURNAL OF APPLIED PHYSICS*, vol. 112, no. 4, pp. 043 916 – 043 916–7, 2012.

[6] A. Bergqvist, "Magnetic vector hysteresis model with dry friction-like pinning," *Physica B: Condensed Matter*, vol. 233, no. 4, pp. 342–347, 1997.

[7] APERAM. [Online]. Available: http://www.aperam.com/en/alloys-amilly/downloads/datasheet/

[8] V. François-Lavet, F. Henrotte, L. Stainier, L. Noels, and C. Geuzaine, "Vectorial incremental nonconservative consistent hysteresis model," in *Proceedings of the 5th International Conference on Advanded COmputational Methods in Engineering (ACOMEN2011)*. Liège, Belgium: ACOMEN2011, November 2011.

[9] F. Henrotte, A. Nicolet, and K. Hameyer, "An energy-based vector hysteresis model for ferromagnetic materials," *COMPEL*, vol. 25, no. 1, pp. 71–80, 2006.

[10] A. Bergqvist, D. Lin, and P. Zhou, "Temperature-dependent vector hysteresis model for permanent magnets," *IEEE Transactions on Magnetics*, vol. 50, no. 2, p. 7008404, 2014.

[11] D. Lin, P. Zhou, and A. Bergqvist, "Improved vector play model and parameter identification for magnetic hysteresis materials," *IEEE Transactions on Magnetics*, vol. 50, no. 2, p. 7008704, 2014.

[12] J. Hopkinson, "Magnetic and other physical properties of iron at a high temperature." *Philosophical Transactions of the Royal Society*, vol. 180, no. 1, pp. 443–465, 1889.

[13] F. Fausto, *Characterization and Measurement of Magnetic Materials*. Academic Press, 2005.

[14] R. Gersdorf, "Ferromagnetic properties of fe and ni in relation to their band structure." *J. Phys. Radium*, vol. 23, no. 10, pp. 726–729, 1962.